Marine Geophysical Research (2022) 43:20
https://doi.org/10.1007/s11001-022-09482-0

ORIGINAL RESEARCH PAPER

A new method for OBS relocation using direct water-wave arrival times from a shooting line and accurate bathymetric data

Hongwei Liu[1] · Huaishan Liu[1,2] · Lei Xing[1,2] · Qianqian Li[1]

Received: 24 December 2021 / Accepted: 2 May 2022 / Published online: 27 May 2022

Abstract

Relocation of the ocean-bottom seismometer (OBS) is a basic step for subsequent inversion of stratigraphic structure. Obtaining sufficient and accurate position information is crucial to the final velocity model. We propose a new OBS relocation method using direct-wave arrival time information and accurate bathymetric data to provide a better starting of seismic velocity tomography. The new method consists of three steps. The first step is to determine the projection position of OBS on the shooting line according to the symmetry of the time-distance curve under the same yaw distance (the distance between ship's position and the shooting line to the left or right). Next, the depth node closest to the observation time is found in the depth profile as the initial position of OBS in the direction perpendicular to the shooting line, based on the projection position. Finally, the final position of the OBS is determined by gradient grid search with the depth node as the center. In this paper, the feasibility of the proposed method is verified by experiments on model data. Then, the method is used to relocate 8 OBSs in the Southwest Pacific Ocean. The results show that the offset between the deployment position and relocation position is 50–500 m, with an average of 206 m.

Keywords OBS relocation · Time-distance curve fitting · Depth profile perpendicular to the shooting line · Gradient grid search

Introduction

Seismic imaging from ocean-bottom seismometers (OBSs) can effectively reveal the deep structure of the marine lithosphere; and provide strong evidence for the study of magmatic activity, hydrothermal cycle mechanisms and the dynamic mechanisms of subduction zone systems (e.g., Watremez et al. 2015; Liu et al. 2020; Sambolian et al. 2021). The first step of using OBS data to invert a high-quality velocity profile is to obtain the exact position of the station (Ao et al. 2010). However, due to the influence of wind and current, the track of the survey vessel does not strictly conform to the planned survey line (Yasukawa and Sakuno 2020), resulting in a deviation between the deployment position of the OBS and the design position. In addition, OBS is affected by ocean currents during descent, increasing the deviation distance (Du et al., 2020). The relocation of the shot points and OBS positions is the basic step for the subsequent study of fine seismic velocity tomography. In the process of data processing, it is crucial to obtain sufficient and accurate position information for the final velocity structure (Zhao et al. 2018).

There are many OBS relocation methods. In the early days, acoustic transceiver systems were the main method for relocating underwater equipment. Creager and Dorman (1982) used acoustic transducers and transponders to reposition OBSs by measuring the distance between the survey ship and subsea equipment at different locations; however, this method required a fixed survey ship to be measured; and thus was time-consuming and imprecise. Osler and Beer (2000) used the Levenberg–Marquardt technique to minimize the summed squared deviation between the known interrogator position and the estimated transponder position and realized the real-time positioning of multiple OBSs

✉ Lei Xing
xingleiouc@ouc.edu.cn

[1] Key Laboratory of Submarine Geosciences and Prospecting Techniques, Ministry of Education, College of Marine Geosciences, Ocean University of China, Qingdao 266100, China

[2] Evaluation and Detection Technology Laboratory of Marine Mineral Resources, Qingdao National Laboratory for Marine Science and Technology, Qingdao 266071, China

by using a towed interrogator transducer. Chen and Wang (2007) used acoustic ranging and GPS positioning to optimize the location of the submarine transponder in shallow water and estimated the average seawater velocity profile. Shiobara (1997) proposed that in addition to acoustic transponders, shot point positions and direct-wave arrival times from OBSs could also be used for repositioning. The method using direct-wave data has become a more efficient method for positioning. Tong et al. (2003) determined the location of OBSs by minimizing the travel time misfit between the observed direct arrivals in the water layer and the travel times modeled by ray tracing and the estimated accuracy of the relocated position was 18 m on the basis of an average travel time residual of approximately 10 ms. Wang et al. (2007) used OBSTOOL (Christeson 1995) software to invert the location of OBS by using the direct-wave arrival time of the vertical component and two horizontal component data. Xue (2008) used trial and error methods to correct the firing time and OBS position. Oshida et al. (2008) searched the bathymetric nodes to obtain the initial value of the nonlinear equation, which effectively avoided the local extremum problem. Ao et al. (2010) used a combination of the least squares and the Monte Carlo method to relocate OBS by using 3D seismic data in the southwestern Indian Ocean. Zhang et al. (2013) designed and developed the positioning support systems of OBS for equipment recovery based on GIS. Han and Wang (2017) used the time slice method to locate Benazzouz et al. (2018) linearized the OBS-positioning problem using multiplexing technology, which only used the shot location and the first arrival times as input data. Du et al. (2018) calculated the OBS position in a 3D seismic survey near the Bashi channel by using a combination of the least squares and Monte Carlo methods. Liu et al. (2019) used a method combining the Global Navigation Satellite System (GNSS) and acoustic technique to accurately locate shallow-water OBS.

However, the final accuracy of OBS positioning is related to many coupling parameters, such as the accuracy of the OBS internal clock, depth near the OBS site, direct-wave arrival data and the average water-wave velocity Wang et al. 2007; Oshida et al. 2008; Manuel et al. 2012). In particular, it is easy to judge the projection position of OBS on the shooting line by using the arrival time information of direct-waves in the relocating process of the 2D shooting line, while the position in the direction perpendicular to the shooting line has great uncertainty (Xue et al. 2008).

To improve the relocation accuracy of OBSs in 2D shooting lines and make full use of available data, we propose a new OBS relocation method that uses direct-wave arrival time data and accurate bathymetric data to determine the location of OBSs. Importantly, we point out the problem of inevitable yaw distance (the distance between ship's position and the shooting line to the left or right) in the 2D seismic experiments. The hyperbolic characteristic of the direct-wave arrival time curve is further defined by the same yaw distance group. Then, the curve fitting method and statistical method are combined to obtain the position along the shooting line. The bathymetric node search and a gradient grid search were performed to obtain the position perpendicular to the shooting direction. The method includes three key steps (Fig. 1), which we describe in detail in the Method. In the sampling rate of 100 Hz, the accuracy in the shooting direction is below 1 m, and the total accuracy is approximately 10 m.

Methods

Processing flow

OBS relocation is systematic, and its accuracy is related to factors such as the shot location, direct-wave arrival time accuracy, average seawater velocity, drifting time of the OBS, and depth near the OBS. The processing flow we use is shown in Fig. 2.

1. The input information is determined: shot point coordinates, direct-wave arrival time, OBS deployment position, and bathymetric data. The average seawater velocity can be calculated from conductivity–temperature–depth (CTD) data or expendable bathythermograph (XBT) data (Del Grosso 1974; Mackenzie 1981); otherwise, the initial velocity is calculated according to the direct-wave curve-fitting process.
2. The input coordinates are rotated so that the parallel and perpendicular components of the shooting line directions can be directly represented by the values of X and Y coordinates, and the rotation angle is determined by the shot point coordinate information according to the least squares method.
3. According to the yaw distance distribution range, the shot point satisfying a certain yaw distance and the corresponding direct-wave arrival time are selected as effective events. After randomly missing some effective events, hyperbolic fitting of the direct-wave arrival time is carried out to obtain the axis of symmetry. Statistical methods are used to determine the maximum probability value as the final projection position. At the same time, many parameters, such as the drifting time of the OBS, the average seawater velocity, the position of the OBS perpendicular to the shooting direction and depth of the OBS, can be obtained. The drifting time and the average seawater velocity are used in the next process.
4. The drifting time in the fitting process is judged. If the value is approximately 0 as the center distribution, the final result which may be a small value is changed to 0,

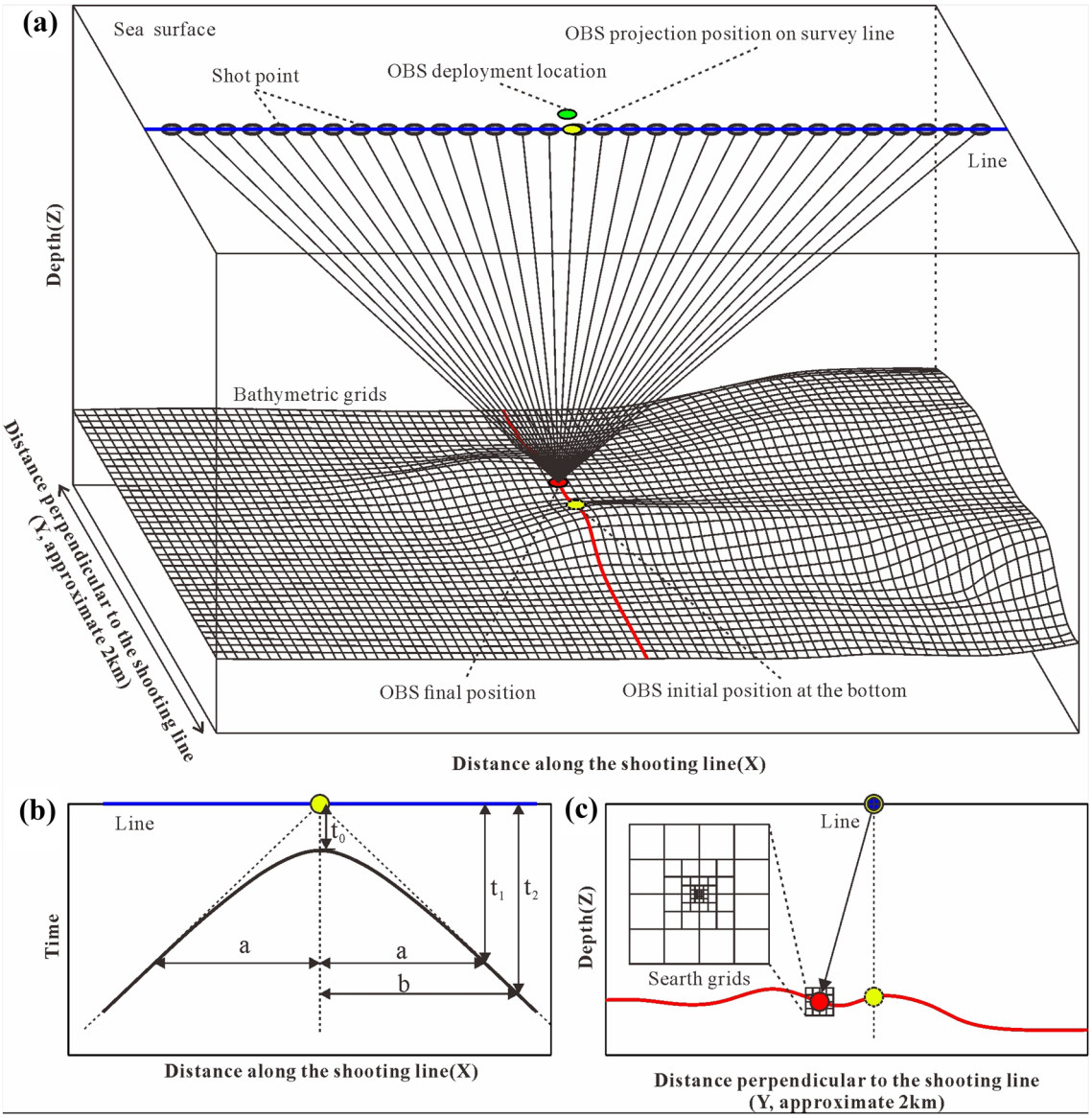

Fig. 1 Schematic diagram of OBS relocation principle. **a** Shows a diagram of the OBS location, shot points and bathymetric grids in space. **b**, **c** Present profiles parallel and perpendicular to the shooting line respectively. The blue line is the shooting line, the red line is the terrain profile perpendicular to the shooting line, the green circle is the deployment position of the OBS, the yellow solid circle is the online distance position of the OBS, the yellow dotted circle is the projection position of the OBS on the seabed, and the red circle is the final position of the OBS

because the OBS does not have a drifting time. If the center of the distribution of the value is not 0, it indicates that the OBS has a drifting time phenomenon. We need to subtract the drifting time from the direct-wave arrival time.

5. According to the projection position, the terrain profile is extracted in the Y direction from the accurate bathymetric data, and each bathymetric node is searched in turn. The node whose theoretical arrival time is closest to the actual arrival time is found as the initial position of the OBS perpendicular to the shooting direction.
6. With the bathymetric node as the center, a gradient grid search is carried out in the profile perpendicular to the shooting line within the accuracy range of the bathymetric data, and the grid spacing is gradually reduced. Stable results, which are the final position of OBSs, are obtained after several iterations.

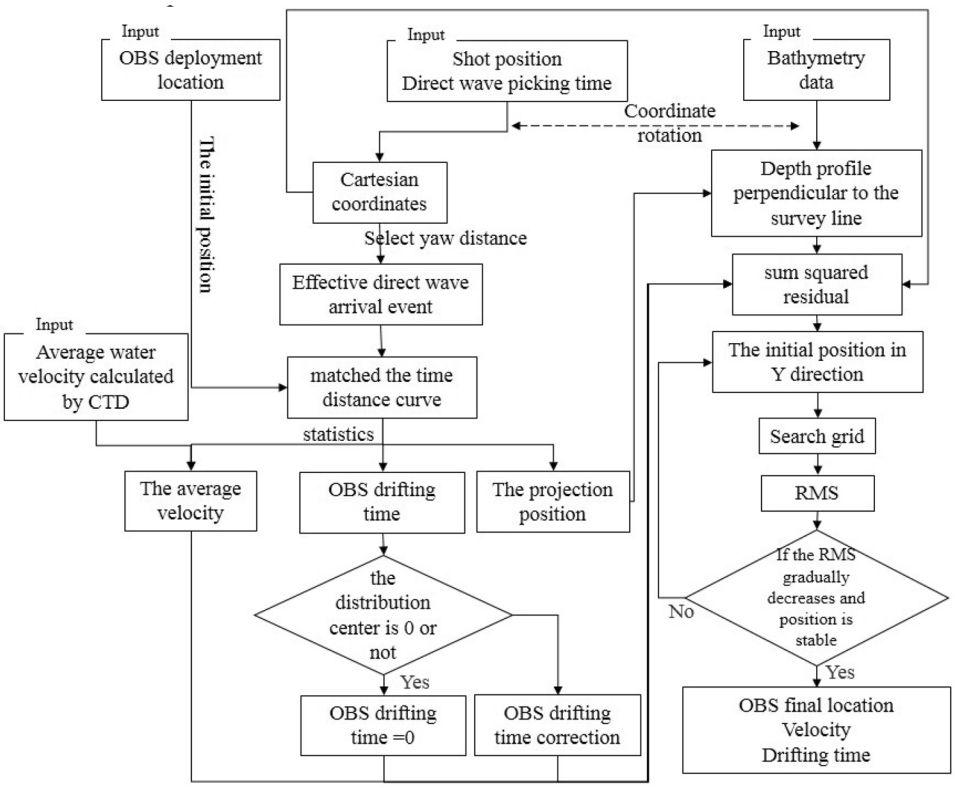

Fig. 2 The processing flow of OBS relocation

Determining the projection position of OBS on the shooting line

The position of an OBS relative to a shooting line can be divided into two parts, as shown in Fig. 1: the online distance along the shooting line (the position in the X direction) and the offset distance perpendicular to the shooting line (the position in the Y direction). According to geometry, the arrival time of direct water waves from the shot point to the OBS can be expressed as follows (Nakamura et al. 1987):

$$t_i = \frac{\sqrt{\left(x_{sp}^i - x_{obs}\right)^2 + \left(y_{sp}^i - y_{obs}\right)^2 + h_{obs}^2}}{v_m}$$

Here, x_{obs}, y_{obs}, and h_{obs} are the positions of the OBS; v_m is the average seawater velocity; and x_{sp}^i and y_{sp}^i are the online distances and yaw distances of each shot point parallel and perpendicular to the shooting line, respectively.

When the OBS is stably located at the bottom of the sea, x_{obs}, y_{obs} and h_{obs} are constants. The lateral variation in the seawater in the same area is small, so the average seawater velocity v_m is relatively stable; therefore, it can also be regarded as a constant. When the yaw distance of the shot point is fixed, the expression can be written as:

$$\begin{cases} \frac{t_i^2}{A} - \frac{\left(x_{sp}^i - x_{obs}\right)^2}{B} = 1 \\ B = \left(y_{sp}^i - y_{obs}\right)^2 + h_{obs}^2 \\ A = \frac{B}{v_m^2} \end{cases}$$

When the yaw distance remains unchanged, the arrival time curve of the direct-wave is only related to the online distance of the shot point on the shooting line, which is a hyperbola with the online distance of the OBS as its axis of symmetry (Fig. 1b).

Considering the drifting time of the OBS, the hyperbolic equation is expressed as:

$$\frac{\left(t_i - dt_{obs}\right)^2}{A} - \frac{\left(x_{sp}^i - x_{obs}\right)^2}{B} = 1$$

In the formula, dt_{obs} is the drifting time of the OBS, which affects the vertex position of the hyperbola.

Therefore, the coordinates of shot points with a smaller yaw distance range and the corresponding direct-wave arrival time can be selected as effective events, and the symmetry axis of the time-distance curve can be obtained as the projection position of the OBS on the shooting line. Combined with actual conditions, the pickup of the direct-water

wave arrival time has uncertainty, and we fit the curve multiple times by randomly missing valid events for each yaw distance range and find the position of the symmetry axis. Finally, statistical methods are used to select the most likely value as the online distance of OBS, that is, the projection position on the shooting line.

Figure 3a is the diagram of the curve fitting process, which shows that the process fit into a time-distance curve based on the direct-wave arrival times. In addition to the projection position, many parameters, such as the drifting time of the OBS, the average seawater velocity, the position of the OBS in the Y direction and depth of the OBS, can be obtained. The drifting time and the average seawater velocity are used in the next process.

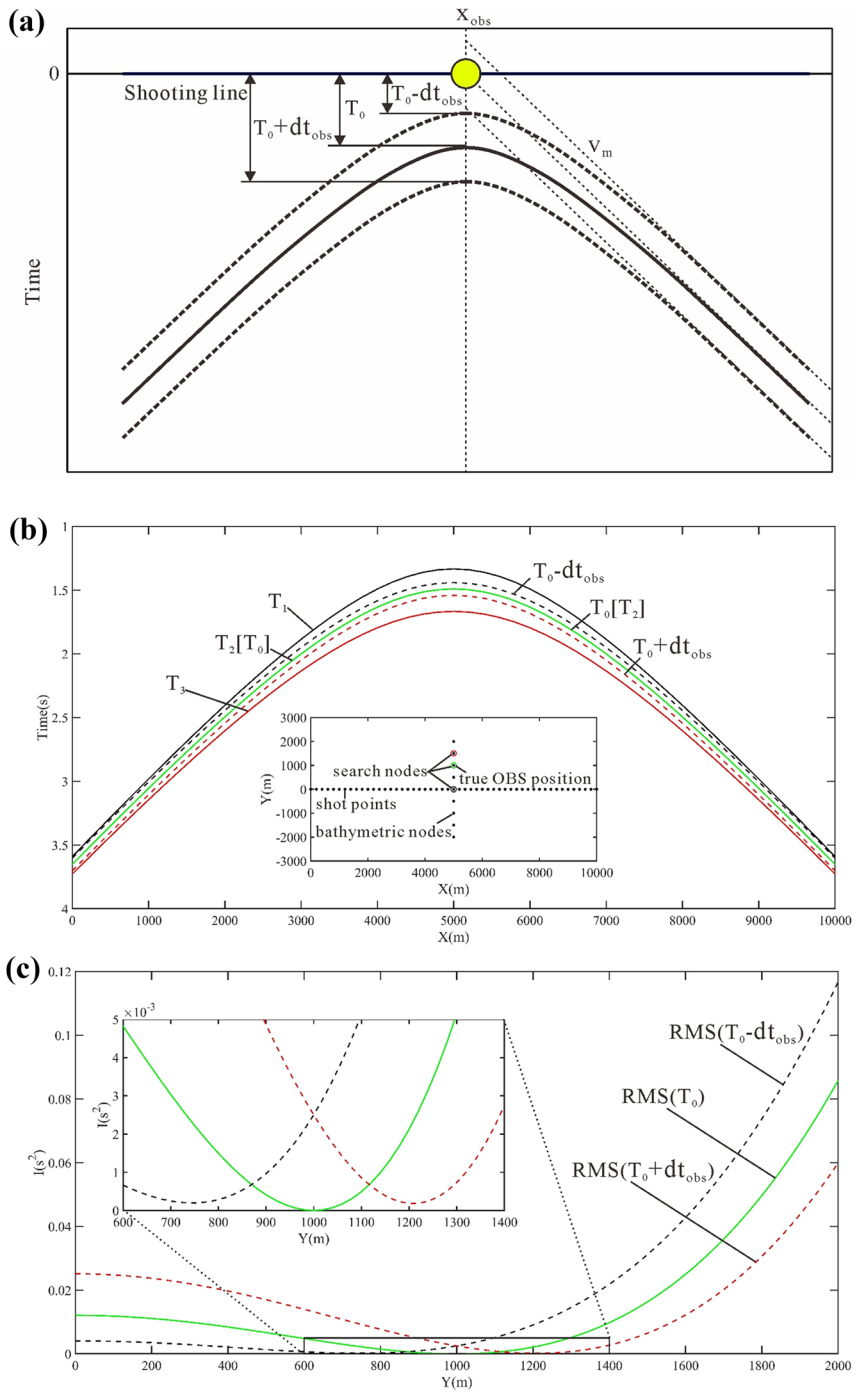

Fig. 3 Diagram of the curve fitting process and the results of the bathymetry node search. **a** Shows the process of the curve fitting; the projection position, the drifting time of the OBS, the average seawater velocity, the distance from OBS to the shooting line can be obtained. **b**, **c** Show the results of the bathymetry node search; **b** is the time-distance curve of 3 search nodes. The geometry can find in the subgraph. The green line is the theoretical arrival time; The dashed lines represent a forward and backward drifting time respectively. c shows the variance between the theoretical and actual time. The green line is the result without drifting time and the dashed lines that the color correspond to **b** are the results with drifting time

Determining the initial OBS position perpendicular to the shooting line

In this section, the initial position in the Y direction is obtained. The specific principle is to find the bathymetric grid node with the best levelling effect of direct water-waves in the terrain profile perpendicular to the shooting line (Han et al. 2017).

In specific calculations, the terrain profile in the Y direction is extracted from the bathymetric data according to the OBS projection position calculated by the previous step. If the projection position is not on the bathymetric grid nodes, the depth is obtained by interpolating the bathymetry between adjacent nodes. All nodes on the profile are taken as the possible positions of the OBS, and the variance between the theoretical and actual time is calculated. The node with the minimum variance is selected as the initial position of the OBS perpendicular to the shooting line. Specific calculations are performed according to the following formula:

$$I_j = \sum_{i=1}^{n} \left(t_i^0 - dt_{obs} - \frac{\sqrt{\left(x_{sp}^i - x_{obs}\right)^2 + \left(y_{sp}^i - y_j\right)^2 + h_j^2}}{v_m} \right)^2$$

In the above formula, x_{sp}^i and y_{sp}^i are the coordinates of the shot points in the X and Y direction, respectively; t_i^0 is the arrival time of the direct water wave corresponding to each shot point; dt_{obs} is the drifting time of the OBS; v_m is the average seawater velocity; n is the number of shot points; x_{obs} is the projection position of the OBS on the shooting line; y_j and h_j are the yaw distance and depth of the bathymetric grid nodes, respectively, whose online distance is x_{obs}; and I_j is the sum squared residual between the theoretical and actual arrival times corresponding to each bathymetric grid node, which is used to measure the levelling effect of the direct water wave. The bathymetric grid node with the smallest I_j is taken as the initial position of the OBS in the Y direction.

Figure 3b and c show the results of the bathymetry node search under horizontal terrain conditions. If the OBS does not have a drifting time, the minimum value of the variance is obtained in the true OBS position. If there is a forward drifting time in the OBS, which means the hyperbola is moving upward, the minimum value will be shifted towards the shooting line. On the other hand, the minimum value will shifted away from the shooting line. Therefore, we need to determine the drifting time of the OBS before the bathymetric grid node is searched.

It is important to note that the drifting time in the fitting process should be judged before bathymetric nodes are searched. If the value is approximately 0 as the center distribution, the final result which may be a small value is changed to 0, because the OBS does not have a drifting time. If the center of the distribution of the value is not 0, it indicates that the OBS has a drifting time phenomenon, in which case we subtract the drifting time from the direct-wave arrival time, which is the second time correction of the OBS.

Determining the final OBS position

With the abovementioned bathymetric grid node as the center, a search grid within the accuracy range of multibeam data is created on the profile perpendicular to the shooting line (Fig. 4). Taking a 50 m water depth grid as an example, the initial search grid spacing is 12.5 m.

The standard deviations between the theoretical direct-wave travel time and observation travel time from each grid point to shot points are calculated:

$$\begin{cases} RMS(k) = \sqrt{\frac{1}{n}\sum_{i=1}^{n}[\Delta t(i,k)]^2}, k = 1,2,3,\cdots,81 \\ \Delta t(i,k) = t_i^1 - \frac{\sqrt{\left(x_{sp}^i - x_{obs}\right)^2 + \left[y_{sp}^i - \left(y_{obs}^0 + dy\right)\right]^2 + \left(h_{obs}^0 + dh\right)^2}}{v_m} \\ dy = A \bullet \Delta y, dh = B \bullet \Delta h \end{cases}$$

In the formula,

$$A = \left(-1, -\tfrac{3}{4}, -\tfrac{1}{2}, -\tfrac{1}{4}, 0, \tfrac{1}{4}, \tfrac{1}{2}, \tfrac{3}{4}, 1\right) \cdot (1,1,1,1,1,1,1,1,1)^T, \quad B = A^T$$

,

The point corresponding to the minimum standard deviation is found. If the point is not a boundary point, it indicates that the search result is relatively stable. The new search center is taken, the grid spacing is reduced by half, and the next search is started. After repeating several times, the final OBS position stabilizes within a small range, and the RMS value stabilizes at a lower standard. If the OBS position is unstable, it indicates that the initial bathymetric grid node is incorrect. The accuracy of the input data, especially the bathymetric grid data, should be checked.

Since the node closest to the OBS is obtained by searching the bathymetric grid nodes one by one perpendicular to the shooting line, the change in each parameter in this step is small, and the local extremum problem is significantly avoided.

The new OBS relocation method we proposed includes three key steps (Fig. 1): (1) Based on the symmetry of the time-distance curve at the same yaw distance, the axis of symmetry of the time-distance curve at a small yaw distance group is obtained, and the position of the OBS in the X direction is determined by using a statistical method. (2) According to the position, the terrain profile in the Y

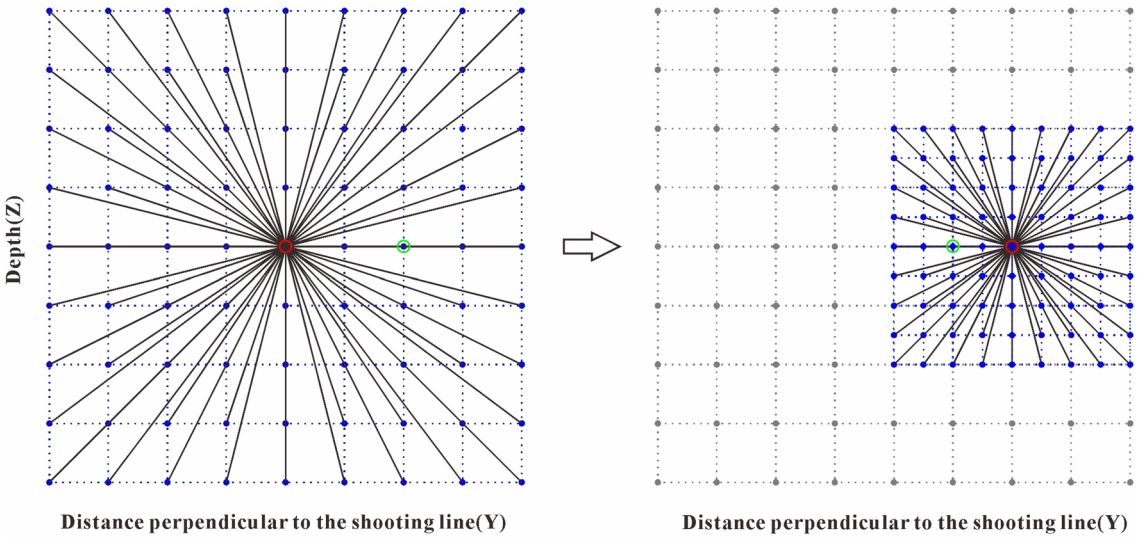

Fig. 4 The diagram of the search grid

direction is extracted from accurate bathymetric data, each bathymetric node is searched in turn, and the node whose theoretical arrival time is closest to the actual arrival time is assigned the initial position of the OBS in the Y direction. (3) With the bathymetric node as the center, a gradient grid search is carried out in the profile perpendicular to the shooting line within the accuracy range of the bathymetric data, and the grid spacing is gradually reduced. Stable results, namely, the final positions of the OBSs, are obtained after several iterations. This method can effectively avoid falling into local minima during the relocation process. By testing large number of models in Sect. 5.3, we summarize the change relationship between the drifting distance range and the sampling frequency. As the sampling frequency increases, the direct-wave arrival time becomes more accurate, and thus, the relocation accuracy increases. At a sampling rate of 50 Hz, the accuracy in the X direction is 0–2.5 m. When the sampling rate is greater than 100 Hz, the accuracy in the shooting direction is below 1 m, and the total accuracy is approximately 10 m.

Model-based testing

The applicability on a shooting line

A theoretical model is used to verify the feasibility of this method. In the actual OBS relocation process, parameters that can be input include the shot point coordinates, direct-wave arrival time, bathymetric grid data, OBS deployment position and recovery position, average seawater velocity and so on. The simulation process should be as accurate as possible to conform to these parameters, especially the shot point coordinates and direct-wave arrival time.

As shown in Fig. 5, we assume that the shooting line in the experiment is 10 km long and that the OBS deployed at a 5000 m distance in X direction has a 100 m distance in Y direction. The number of shot points is 400, separated by an interval of 25 m. The multibeam sweep range is 2000 m, and the reference water depth of the horizontal terrain with a 100 m vertical dip height is 2000 m. The average seawater velocity is 1500 m/s. To conform to the track of the investigated ship in the actual construction process, the maximum yaw distance is set as 25 m. According to the above geometry, the theoretical arrival time of the direct-wave is calculated by the ray method. Random errors consistent with a normal distribution are added to the theoretical data to conform to the distribution of picking uncertainties, and the error range is set to 20 ms.

After the observation data are prepared, the relocation method mentioned above is used for relocation. We divide the yaw distance into five groups, approximately 80 shot points per group, and we obtain a stable result. We examine the influence of the yaw distance range in Sect. 5.2 and verify that the minimum yaw distance group that can obtain the stable result is 5 m in this model. The relocation process is shown in Fig. 6, and the final parameters are shown in the first row of Table 1. In the X direction, 5 groups of yaw distances are selected to fit the time-distance curve to obtain the symmetry axis (Fig. 6a). For a single yaw distance group, the maximum deviation compared with the theoretical position is 2.26 m, and the minimum deviation is 0.08 m. The average position of the OBS is 0.42 m longer than the theoretical position. In the Y direction, the results of positions are stable in a small range (Fig. 6b, c). The final position is

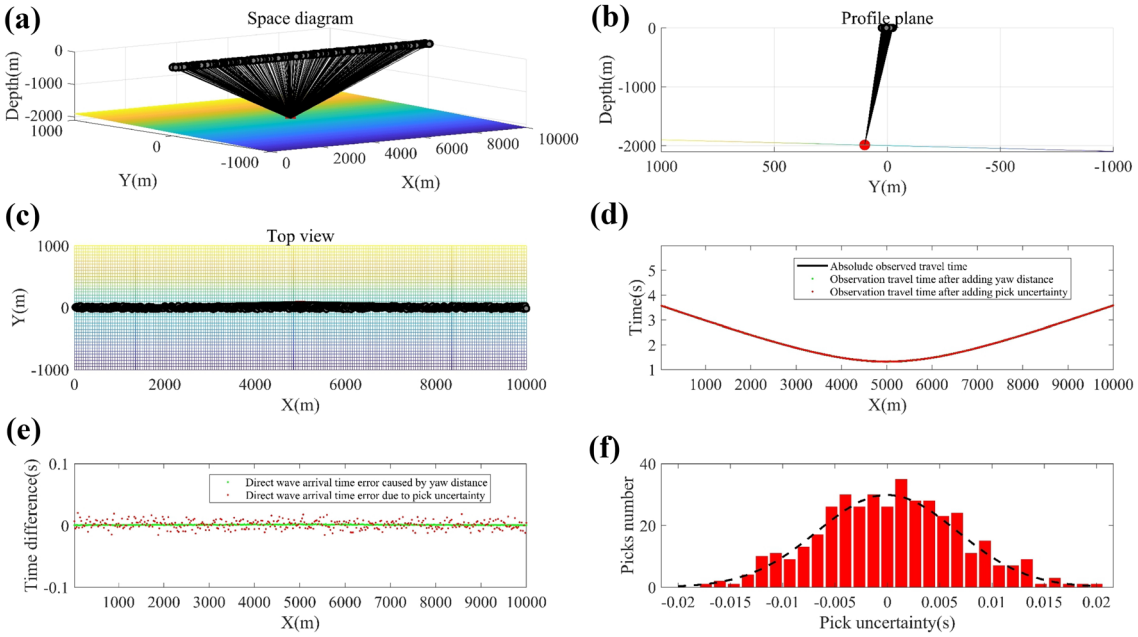

Fig. 5 Diagram of the theoretical model. **a–c** Are the space diagram, profile plane and top view of the model, respectively; **d** is the simulated direct-wave arrival time; **e** is the direct-wave arrival time error caused by deviations in the Y direction and pick uncertainties; and **f** is the distribution of picking uncertainties. The red rectangular columns represent the number of picking uncertainties. The black dotted line represents a Gaussian distribution

Table 1 The correction results and parameters of different picking uncertainties

Picking uncertainty(s)	OBS theoretical location		Corrected location			Seawater velocity (m/s)	Drifting distance (m)	RMS (ms)
	X (m)	Y (m)	X (m)	Y (m)	Dep (m)			
0.02	5000	100	5000.42	97.66	− 1987.89	1500.13	2.38	16.67
0.03	5000	100	5001.01	89.06	− 1988.14	1500.42	10.98	45.29
0.04	5000	100	4999.68	144.53	− 1983.38	1499.81	44.53	70.53

97.66 m, which indicates that the difference compared with the theoretical value is only 2.34 m. The relocation accuracy in the X direction is high, and the relocation result in the Y direction is also good. The inversion results can restore the position of the OBS. More importantly, the value of the sum squared residuals (Fig. 6d) of the final iteration is 16.67 ms, which is almost the same as that with 20 ms of picking uncertainty is added. Hence, this method is feasible and effective for relocating OBS.

The applicability on 2 shooting lines

A good method should have good universality, and the applicability of this method is tested with simulated data on 2 shooting lines. Assuming that there are two perpendicularly intersecting shooting lines with azimuths of 0 and 90, the number and interval of shot points are consistent with the above model verification. The seabed topography is horizontal in the X direction and inclined in the Y direction (Fig. 7). We select different OBS points to calculate direct-wave arrival times (Fig. 7a2, b2, and c2) and use this method for relocation. In the process of curve fitting of the direct-wave arrival time in the first step and water depth node search in the second step, the data in the X direction are selected. In the process of gradient grid search in the third step, the data in the Y direction are used. The relocation results are shown in Fig. 7, and the detailed parameters are shown in Table 2. The accuracy of the Y direction is greatly improved and can be consistent with that of the X direction. Therefore, this method can also be used with data on 2 shooting lines and has good universality.

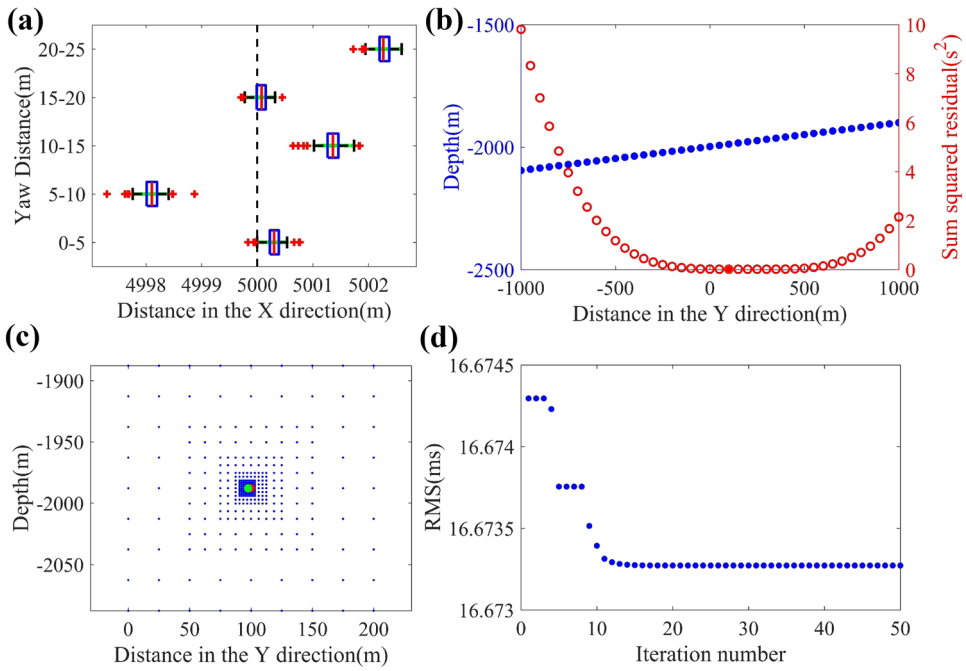

Fig. 6 Relocation process and results for the theoretical test. **a** Shows the relocation results in the X direction. The black dashed line represents the theoretical position in the X direction. The green dot is the position of the symmetry axis of the hyperbola fitting. A normally distributed box line is drawn on the green dots, the red line is the statistical position of the yaw distance group, and the red plus signs on both sides represent the singularity. **b** Shows preliminary relocation results in the Y direction. The blue dots represent the terrain profile perpendicular to the shooting line, and the red open circles represent the sum squared residuals corresponding to the bathymetric grid nodes. The red solid circle is the minimum node of the calculation, and this node is the initial position of the OBS. **c** Shows the gradient grid search results centered on the initial position. The blue dot is the grid point, the red dot is the initial position and the green dot is the final position. **d** Represents the relationship between the RMS travel-time error and the number of iterations

Table 2 The correction results and parameters for different OBS positions on 2 shooting lines

Serial number	OBS theoretical location		Corrected location			Seawater velocity (m/s)	Drifting distance (m)	RMS (ms)
	X (m)	Y (m)	X (m)	Y (m)	Dep (m)			
1	5000	100	4999.90	99.83	− 1997.28	1499.83	0.20	17.22
2	4500	500	4499.96	500.12	− 1990.11	1500.21	0.13	17.93
3	4000	1000	4001.15	1000.44	− 1979.69	1499.96	1.23	19.58

Application of OBS relocation

In early 2021, Ocean University of China carried out an active source OBS seismic survey to obtain the mid-deep velocity structure beneath the western Melanesian Trench (WMT) northeast of New Guinea (Fig. 8). The shooting line was 185 km long, and the distribution interval of the 8 OBSs was 10–30 km. A large-capacity air gun with 8000 Cu.in was used as the source, and the excitation interval was 90 s. The source was excited along the shooting line, and multibeam bathymetric measurements were carried out synchronously. The ship's position was determined by onboard GPS, which accurately recorded the firing time of the air gun. The accurate bathymetric data extracted from multibeam data and the direct-wave arrival time data picked from OBS data were used for OBS relocation. Figure 8 and Table 3 show the relocation results and parameters of the 8 OBSs. The results show that the deviation between the deployed location and the corrected location was 50–500 m and the average deviation was 206 m.

Station A1 is taken as an example to show the relocation effect of this method. First, the OBS data are converted into a common receiver point gather according to the firing time of the air gun. The reduction velocity is not used to show the symmetric form of the direct-wave. Then, input data for the

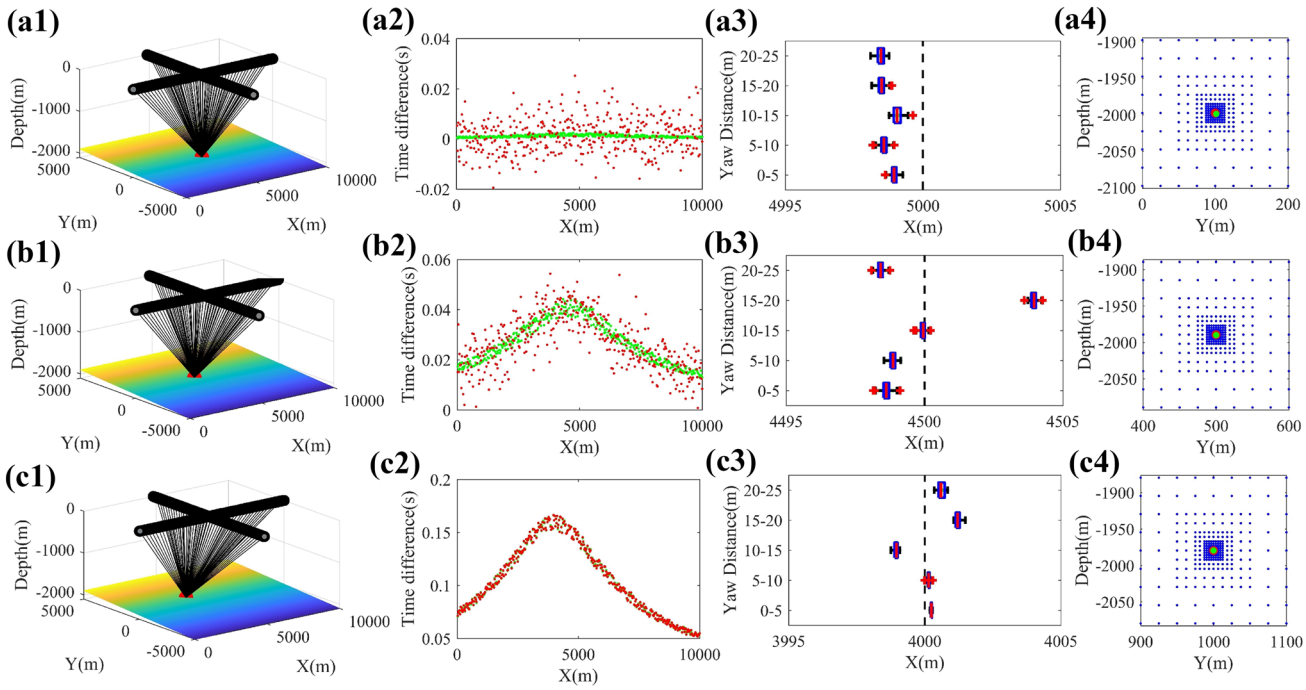

Fig. 7 The model and relocation results on 2 shooting lines. **a1**, **b1** and **c1** Show diagrams of the geometry at 3 different OBS positions. **a2**, **b2** and **c2** Show the differences between the simulated direct-wave arrival times and error-free arrival times (green dots represent the direct-wave arrival time error caused by the yaw distance, and red dots represent the direct-wave arrival time error due to picking uncertainties). **a3**, **b3** and **c3** Show the relocation results in the X direction (the black dsshed line represents the theoretical position in the X direction, the green dots are the positions of the symmetry axis of the hyperbola fitting, on which a normally distributed box line is drawn, the red line is the statistical position under the yaw distance, and the red plus signs on both sides represent the singularity). **a4**, **b4** and **c4** show the gradient grid search results centered on the water depth node (the blue dot is the grid point, the red dot is the initial position, and the green dot is the final position)

relocation method are prepared, including the picked direct-wave arrival times and the bathymetric grid data extracted from multibeam data based on the deployment location. Next, this method is used for OBS relocation, and the results are shown in Fig. 9. In the positioning process, only one yaw distance group with the maximum probability is selected according to the yaw distance of the shot point to ensure sufficient effective event data of the direct-wave arrival times. Figure 9a shows the relocation results in the X direction. The fitted coordinate axes are distributed between 11013.40 and 11017.15 m, indicating that all positions are stable within a range of less than 4 m. The final result in the X direction is 11015.41 m. Figure 9b and c show the preliminary and final relocation results in the Y direction, respectively. The red dot is the initial position, which is a specific node in the bathymetric grid, while the green dots are the final relocation positions after the gradient grid search iteration. The position is stable after gradient grid search. The RMS trend decreases with the number of iterations and finally stabilizes at 15.12 ms (Fig. 9d).

As shown in Fig. 10, the linear normal moveout (NMO) of the OBS data is performed by using the coordinates before and after OBS relocation. Whether the direct-wave can be flattened represents whether the relocation effect is good. It can be seen that, the direct waveform state of linear NMO after relocation (Fig. 10b) is basically a straight line, while the direct waveform state of linear NMO before relocation (Fig. 10a) is not horizontal. This also justifies the accuracy of the OBS relocation.

Discussion

OBS relocation is a systematic process, and the OBS position is related to the depth near the OBS station, the accuracy of the direct-wave arrival time data picked and the accuracy of the OBS internal clock. Next, we discuss the influence of input parameters such as depth, yaw distance range and picking uncertainty on OBS relocation.

The influence of bathymetric grid data

This method is proposed for OBS relocation in 2D shooting lines. In the process of obtaining the OBS position in the X direction, only the symmetry of the time-distance curve with the same yaw distance is considered, and other factors

Table 3 The OBS locations and parameters before and after correction

OBS station	Deployed location		Cartesian coordinates after rotation		Corrected location			Seawater velocity (m/s)	Drifting distance (m)	RMS (ms)	Drifting time (s)
	E	N	X (m)	Y (m)	X (m)	Y (m)	Dep (m)				
A1	542628.21	9669149.42	10949.33	− 50.79	11015.41	− 207.49	− 2042.23	1500.26	170.06	15.12	− 0.5872
A2	551186.17	9677484.25	22895.37	− 37.24	22799.85	− 140.51	− 2799.11	1498.60	140.68	28.12	− 0.9349
A3	559742.51	9685823.80	34843.54	− 19.17	34742.89	24.13	− 2938.69	1499.42	109.57	11.13	− 0.8131
A4	568408.58	9694198.86	46895.15	− 52.11	46869.14	− 177.08	− 3330.62	1501.83	127.64	12.51	− 0.5960
A5	587064.04	9712278.17	72873.73	− 86.94	72848.60	370.17	− 3680.32	1500.43	457.81	13.27	− 0.6038
A6	597071.16	9722034.55	86849.74	− 63.80	86835.34	− 113.09	− 3391.57	1500.68	51.35	11.37	− 0.5957
A7	609187.27	9733861.43	103781.18	− 25.49	103841.61	− 377.62	− 3130.78	1499.14	357.28	12.08	− 1.0271
A8	629163.44	9753308.19	131659.90	− 0.01	131674.36	− 237.21	− 3057.72	1499.37	237.64	14.80	− 0.9381

are irrelevant. Therefore, the bottom topography does not affect the relocation results in the X direction. The process of obtaining the OBS position in the Y direction is divided into two parts. First, a node is determined according to the bathymetric grid data, and then the final position is determined by a small-scale gradient grid search centered on the node. Therefore, the bathymetric grid data affect the relocation results of the Y direction.

For horizontal terrain, there is no elevation difference in the Y direction. When we use the 2D data for OBS relocation, there are two symmetric nodes about the shooting line to make the direct-wave leveling effect best, except that OBS is right on the line. Further constraint by the data outside the shooting line is necessary to obtain an accurate position and avoid this theoretical error.

As shown in Fig. 11a, we select three shooting lines to illustrate the theoretical error in horizontal terrain and test the effect of a point data outside the shooting line in the OBS relocation process. Figure 11b and d shows the variance between the theoretical and actual times of all bathymetric nodes in the terrain profile perpendicular to the shooting line. The solid line is the result of a shooting line and the line of open circles is the result that adds the point data outside the shooting line. The subgraph is a larger display of the black rectangle in each diagram. As we can see from Fig. 11b, when the OBS is right on the shooting line, there is only one minimum point that corresponds to the theoretical position of the OBS. The solid lines in Fig. 11c and d are symmetrical curves and their axis of symmetry is the location of the shooting line. There are two minimum points, which correspond to the theoretical position and mirror position of the OBS. The line of open circles has no symmetry, and the corresponding node of the theoretical position of the OBS is the minimum. The non-uniqueness of the OBS position in the horizontal terrain is overcome by adding the data outside the shooting line.

According to the relocation principle, this method is more suitable for situations with large fluctuations in the seafloor. For the actual seafloor, the initial position can be confirmed more accurately when the bathymetric node search is carried out in the Y direction as the terrain is irregular.

In general, the multibeam measurement accuracy is approximately 10 m (5‰ water depth, calculated at a 2000 m water depth), and the transverse node spacing is approximately 50 m (Maleika 2020). This is also the reason why we further limited the possible errors in the Y and depth directions in the final gradient grid search. If the error of the initial node caused by the low accuracy of bathymetric grid data is too large, the results of the gradient grid search become unstable (Fig. 12).

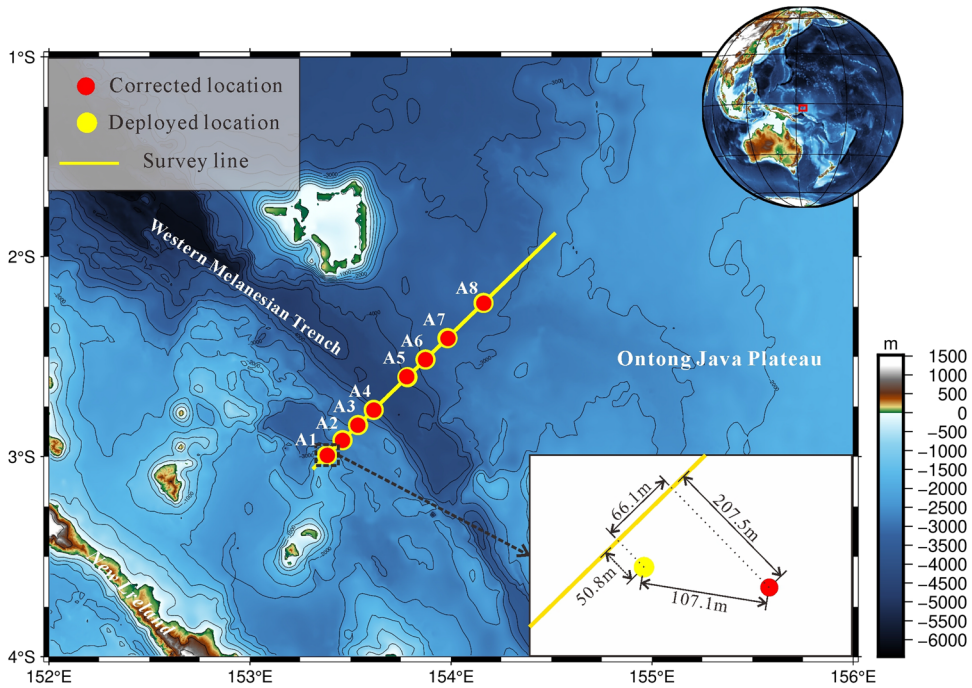

Fig. 8 Relocation results of 8 OBSs in the WMT. The solid yellow line is the shooting line. The yellow and red dots represent the deployed and corrected locations, respectively

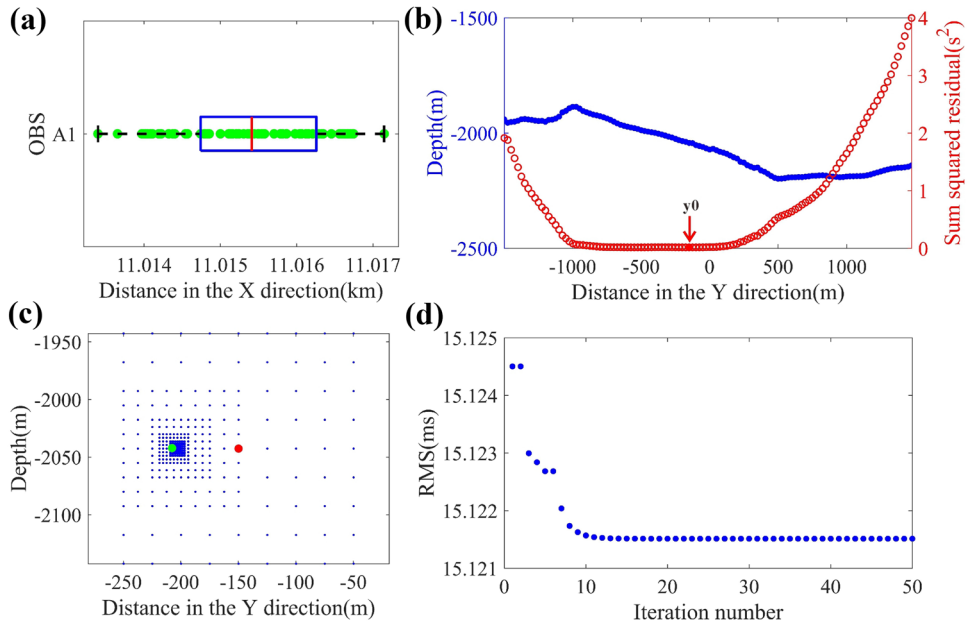

Fig. 9 Relocation process and results taking Station A1 as an example. **a** Shows the relocation results in the X direction. **b**, **c** Show the preliminary and final relocation results in the Y direction, respectively. The red dots represent the initial OBS location along the Y direction. **d** Represents the relationship between the RMS and the number of iterations

The influence of the yaw distance range

A sufficient quantity of direct-wave arrival times is a prerequisite for the stability of the curve when using the curve fitting method. The same yaw distance data are the best choice, which can only be satisfied in the model. In fact, the yaw distance is a set of changes that have a certain range. Therefore, in the OBS relocation process, the first step is to select effective data through the smaller yaw distance range. The size of the range determines the number of direct-wave arrival times that are fitted to the curve.

Figure 13 shows the results of the curve fitting in different yaw distance ranges. The distribution area of the symmetry axis of the fitting curve decreases as the range increases. There are fewer effective data points in the small yaw distance range, and thus, the result of the curve fitting is not stable. There are more effective data in the large yaw distance range, and the curve fitting result is stable, but if the range is too large, it may lead to a fixed deviation. Therefore, it is

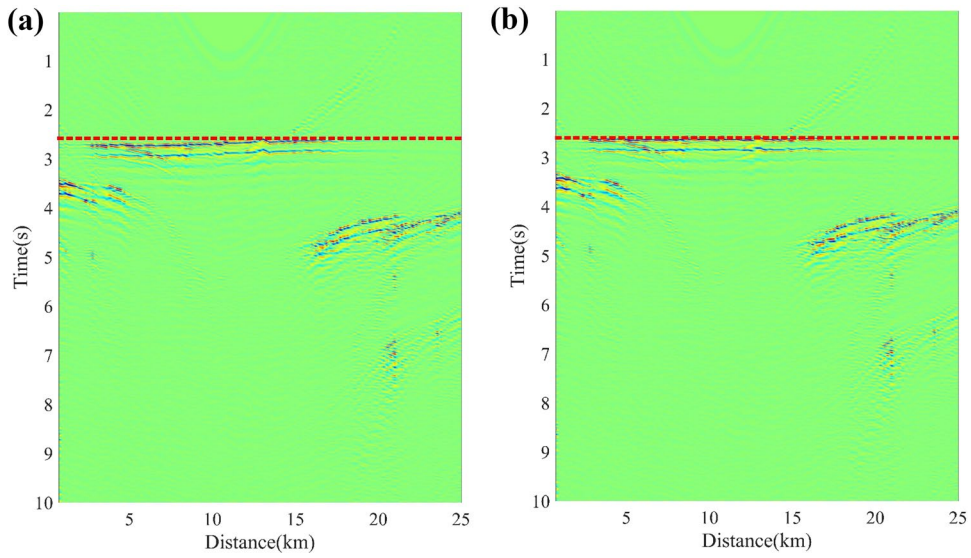

Fig. 10 Comparison of direct-waves of linear NMO before and after OBS relocation taking Station A1 as an example. **a** Shows the result before OBS relocation and **b** shows the result after OBS relocation

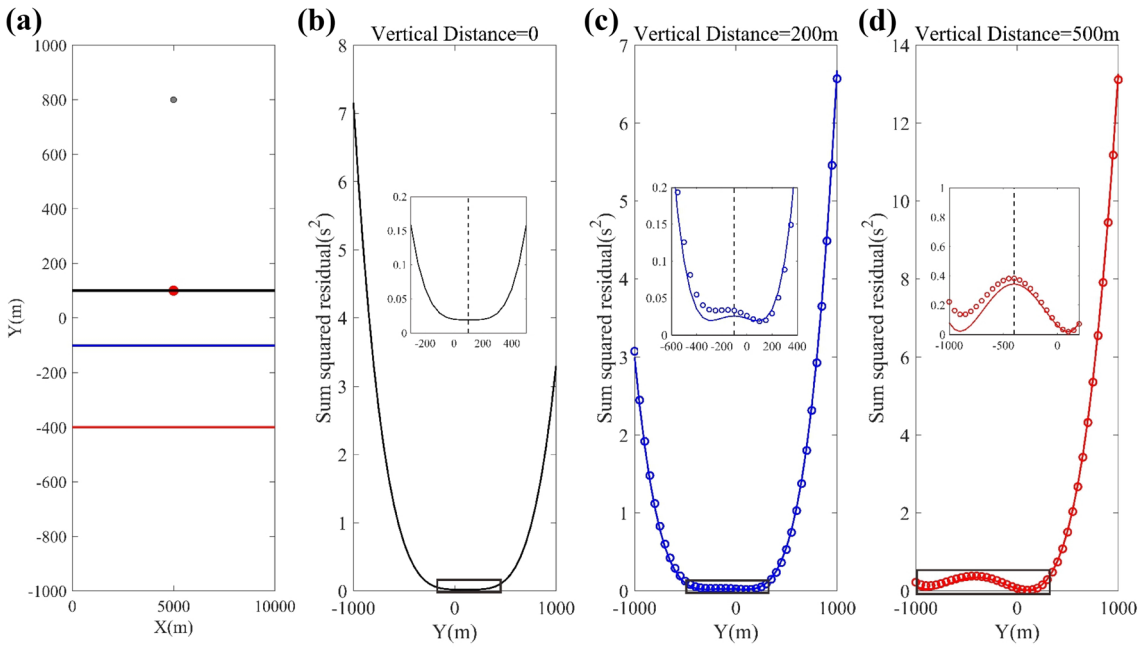

Fig. 11 The search results of bathymetric nodes in horizontal terrain. **a** Shows a schematic of the geometry. The red dot is the theoretical position of the OBS, and the gray dot is the shot point outside the line. The black line, blue line and red line are three shooting lines. **b–d** are the variances between the theoretical and actual times of all bathymetric nodes in the terrain profile. The color represents the same color line in (**a**). The solid line is the result of a shooting line, and the line of open circles is the result that adds the point data outside the shooting line. The subgraph is a larger display of the black rectangle in each diagram

necessary to choose a suitable yaw distance range, not only to obtain stable results but also to obtain relatively accurate results. In the model test, there are 400 shot points with a maximum yaw distance of 25 m. We divide the yaw distance into five groups, approximately 80 shot points per group, and we obtain a stable result. In other words, the minimum yaw distance group that can obtain the stable result is 5 m.

In the actual data processing, we recommend that a larger yaw distance range be selected for curve fitting. Then, the range can gradually be narrowed. Finally, a minimum yaw distance range that can obtain a stable result is selected and the corresponding curve fitting result is the projection position of the OBS on the shooting line.

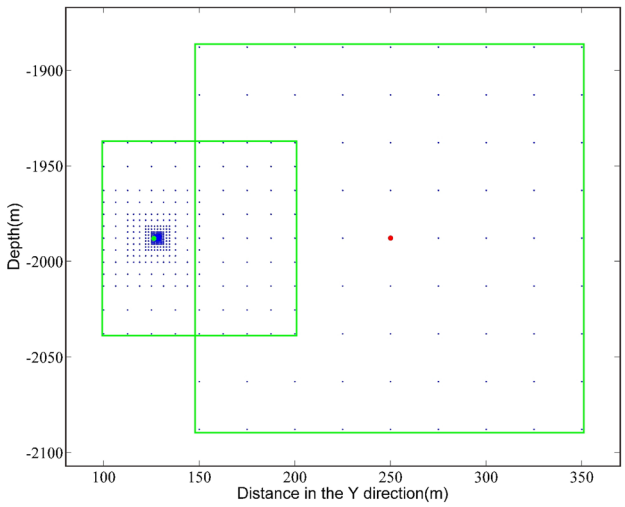

Fig. 12 Unstable search results of gradient grid nodes caused by incorrect bathymetric nodes. The blue dot is the grid point, the red dot is the initial position, and the green dot is the final position. The green square represents the first and second search range, and the error of the initial bathymetric node leads to the second search range beyond the initial search range

The influence of picking uncertainty

The picking uncertainty of the direct-wave arrival time is related to the signal-to-noise ratio of the OBS data, the visual detection difference of the arrival picking and the picking method (Senkaya and Karsli 2014). The error calculated at a sampling rate of 50 Hz is 30 ms, including a digital uncertainty error of 10 ms. We tested the relocation results with uncertainties of 30 ms and 40 ms in the picked direct-wave arrival times and compared them with the relocation result with 20 ms picking uncertainty in the model testing. The relocation results are shown in Figs. 14 and 15, and the parameters are shown in Table 1. The distance between the OBS relocation position and the theoretical position gradually increases with increasing picking uncertainty.

To evaluate the accuracy of the relocation in the proposed method, multiple times of the picking uncertainty consistent with a normal distribution are added to the theoretical direct-wave arrival time. Our method is used for relocation and the drifts in the X and Y directions are calculated. The picking uncertainty is determined by the sampling frequency and each frequency is calculated 30 times. The result is shown in Fig. 16. Overall, the accuracy of the relocation in the X direction is approximately 10 times than in Y direction and the accuracy of relocation rises as the sampling frequency increases. When the sampling rate is lower than 50 Hz, the rate of change of the relocation result is large. When the sampling rate is above 50 Hz, the results are more stable. At a sampling rate of 50 Hz, the accuracy in the X direction is 0–2.5 m. When the sampling rate is greater than 100 Hz, the accuracy in the X direction is less than 1 m.

Conclusions

OBS relocation is a basic step for the subsequent inversion of stratigraphic structure. Obtaining sufficient and accurate position information is crucial to the final velocity model (Zhao et al. 2018). To improve the relocation accuracy of OBS and make full use of available data, we propose a new OBS relocation method, which uses direct-wave arrival time data and accurate bathymetric data to determine the position of OBS. This method consists of three key steps. The first step is to determine the projection position of the OBS in the X direction according to the symmetry of the

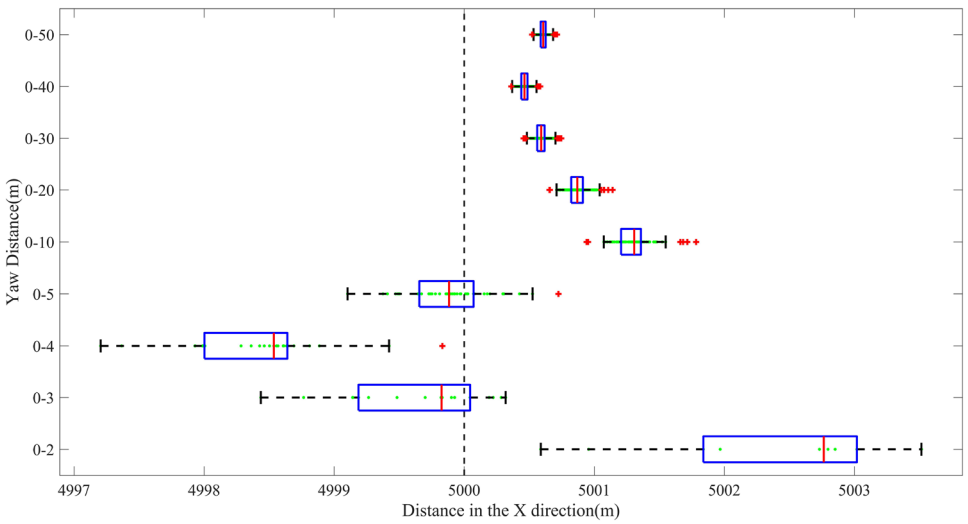

Fig. 13 The results of curve fitting in different yaw distance ranges. The green dot is the position of the symmetry axis of the hyperbola fitting. A normally distributed box line is drawn on the green dots, the red plus signs on both sides represent the singularity, and the red line is the statistical position of the yaw distance group, which is the relocation result of the range

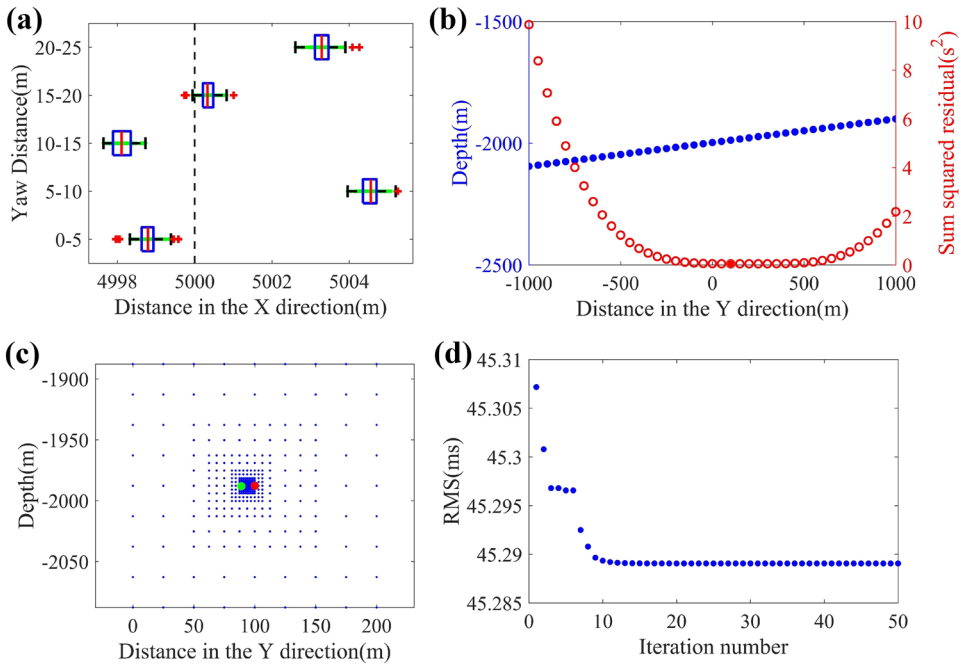

Fig. 14 OBS relocation results with a picking uncertainty of 30 ms

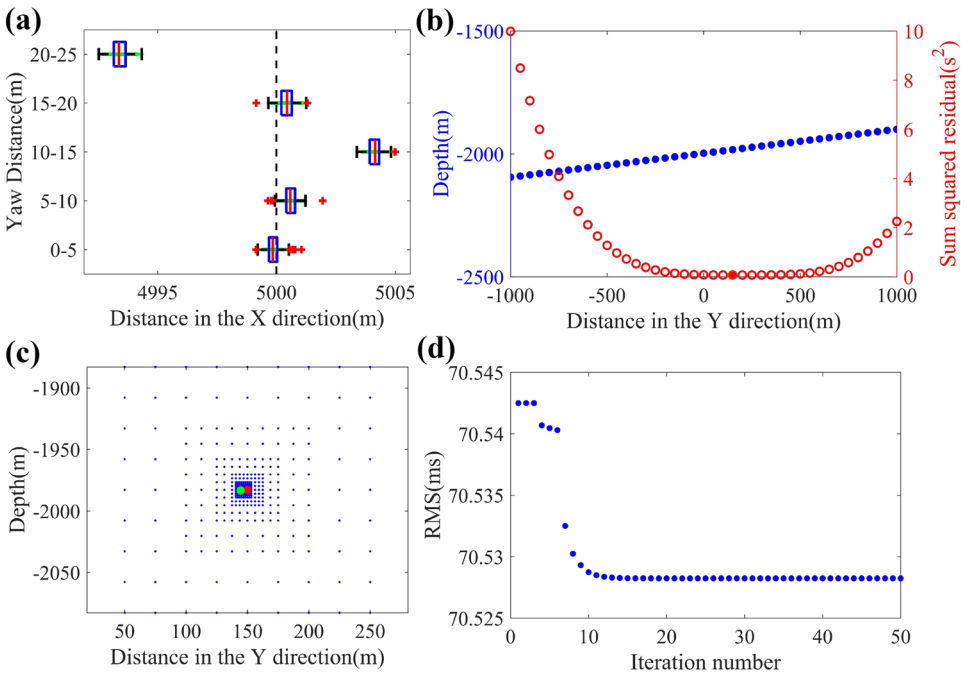

Fig. 15 OBS relocation results with a picking uncertainty of 40 ms

time-distance curve under the same yaw distance. Next, the depth node closest to the observation time is found in the depth profile perpendicular to the shooting line as the initial position of OBS in the Y direction, based on the projection position. Finally, the final position of the OBS is determined by a gradient grid search with the depth node as the center. The above steps can effectively avoid the problem of falling into local minima.

Theoretical model tests show that the proposed method is reasonable and feasible, and this method is applied to the relocation of 8 OBSs in the WMT. We report the following conclusions:

1. The direct-wave arrival time curve under the same yaw distance group is a hyperbola with the OBS online distance as its axis of symmetry. Fitting the direct-wave arrival time curve along a shooting line with a small yaw

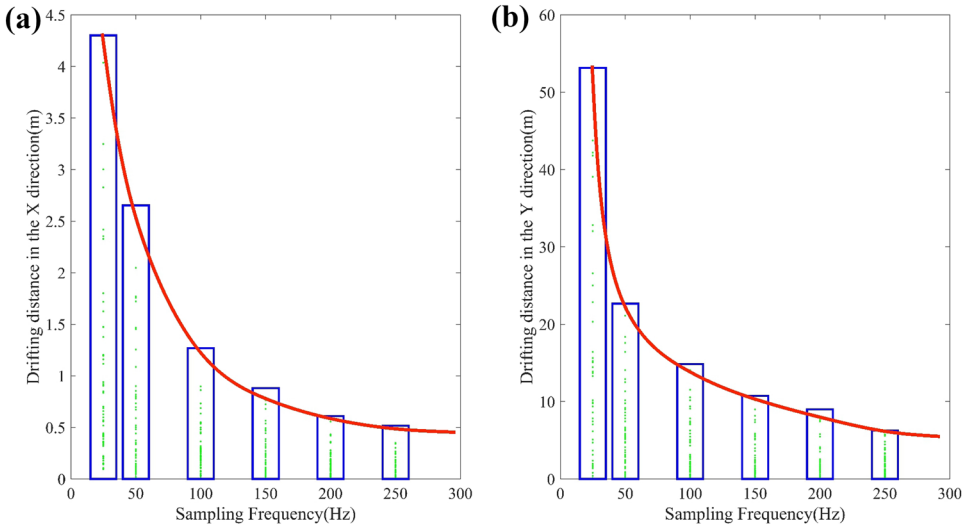

Fig. 16 The drifting distances in X and Y directions at different sampling frequency. The green dot is the drifting distance of a single time, the blue rectangle is the distribution, and the red line is the trend line of the maximum drift

distance is an effective means to obtain the OBS online distance. The relocation results of the OBS projection position on the shooting line are highly accurate, as only the symmetry of the time-distance curve is used, which avoids the interference of other factors.

2. Considering irregular seabed topography can improve the accuracy of OBS relocation and avoid theoretical error of using the direct-wave arrival time on 2D shooting lines.
3. The picking uncertainty of direct-wave arrival time affects the relocation results of OBS. With increasing picking uncertainty, the error increases gradually. However, this error arises mainly in the direction perpendicular to the shooting line and has little influence on the accuracy parallel to the shooting line.
4. This method can not only solve the OBS relocation problem on 2D shooting lines but also be conveniently and quickly applied to data on 2 shooting lines, which indicates that this method has good universality.

Acknowledgements Data and samples were collected onboard of R/V "Kexue", implementing the open research cruise NORC2020-581 supported by NSFC Shiptime Sharing Project (Project Number: 41949581), and Major Research Plan on West-Pacific Earth System Multispheric Interactions (Project Number: 91858215, 91958206), and the Key Research and Development Program of Shandong Province (Grant No. 2019GHY112019).

References

Ao W, Zhao MH, Qiu XL, Li JB, Zhang JZ (2010) The correction of shot and OBS position in the 3D seismic experiment of the SW Indian Ocean Ridge. Chin J Geophys 53(6):1072–1081. https://doi.org/10.1002/cjg2.1577

Benazzouz O, Pinheiro LM, Matias LM, Afilhado A, Herold D, Haines SS (2018) Accurate ocean bottom seismometer positioning method inspired by multilateration technique. Math Geosci 50(5):569–584

Chen HH, Wang CC (2007) Optimal localization of a seafloor transponder in shallow water using acoustic ranging and GPS observations. Ocean Eng 34(17–18):2385–2399. https://doi.org/10.1016/j.oceaneng.2007.05.005

Christeson G (1995) OBSTOOL: software for processing UTIG OBS data. Institute for Geophysics, Austin

Creager KC, Dorman LM (1982) Location of instruments on the seafloor by joint adjustment of instrument and ship positions. J Geophys Res Solid Earth 87(B10):8379–8388. https://doi.org/10.1029/JB087iB10p08379

Del Grosso VA (1974) New equation for the speed of sound in natural waters (with comparisons to other equations). J Acoust Soc Am 56(4):1084–1091. https://doi.org/10.1121/1.1903388

Du F, Zhang J, Yang F, Zhao M, Wang Q, Qiu X (2018) Combination of least square and Monte Carlo methods for OBs relocation in 3D seismic survey near Bashi channel. Mar Geodesy 41(5):494–515. https://doi.org/10.1080/01490419.2018.1479993

Han Y, Wang X (2017) Relocating ocean-bottom seismometers. Indian J Mar Sci 46(3):462–465

Liu H, Wang Z, Zhao S, He K (2019) Accurate multiple ocean bottom seismometer positioning in shallow water using GNSS/acoustic technique. Sensors 19(6):1406. https://doi.org/10.3390/s19061406

Liu B, Wang X, Xu Y, Wen P, Li L, Zhang H (2020) A complex gas hydrate system imaged jointly using MCS and OBS data from the northern South China Sea. Mar Geophys Res 41(4):1–15

Mackenzie KV (1981) Nine-term equation for sound speed in the oceans. J Acoust Soc Am 70(3):807–812. https://doi.org/10.1121/1.386920

Maleika W (2020) Inverse distance weighting method optimization in the process of digital terrain. Appl Geomat 12(4):397–407. https://doi.org/10.1007/s12518-020-00307-6

Mànuel A, Roset X, Rio JD, Toma DM, Carreras N, Panahi SS, Cadena J (2012) Ocean bottom seismometer: design and test of a measurement system for marine seismology. Sensors 12(3):3693–3719. https://doi.org/10.3390/s120303693

Nakamura Y, Donoho PL, Roper PH, McPherson PM (1987) Large-offset seismic surveying using ocean-bottom seismographs

and air guns: instrumentation and field technique. Geophysics 52(12):1601–1611

Oshida A, Kubota R, Nishiyama E, Ando J, Kasahara J, Nishizawa A, Kaneda K (2008) A new method for determining OBS positions for crustal structure studies, using airgun shots and precise bathymetric data. Explor Geophys 39(1):15–25. https://doi.org/10.1071/EG08005

Osler J, Beer J (2000) Real-time localization of multiple acoustic transponders using a towed interrogation transducer. IEEE Xplore 1:725–732. https://doi.org/10.1109/OCEANS.2000.881338

Sambolian S, Gorszczyk A, Operto S, Ribodetti A, Tavakoli F, B (2021) Mitigating the ill-posedness of first-arrival traveltime tomography using slopes: application to the eastern Nankai Trough (Japan) OBS data set. Geophys J Int 227(2):898–921. https://doi.org/10.1093/gji/ggab262

Senkaya M, Karsli H (2014) A semi-automatic approach to identify first arrival time: the cross-correlation technique (CCT). Earth Sci Res J 18(2):107–113

Shiobara H, Nakanishi A, Shimamura H, Mjelde R, Kanazawa T, Berg EW (1997) Precise positioning of ocean bottom seismometer by using acoustic transponder and CTD. Mar Geophys Res 19(3):199–209

Tong CH, Barton PJ, White RS, Sinha MC, Singh SC, Pye JW, Orcutt JA (2003) Influence of enhanced melt supply on upper crustal structure at a mid-ocean ridge discontinuity: a three-dimensional seismic tomographic study of 9° N East Pacific Rise. J Geophys Res Solid Earth. https://doi.org/10.1029/2002JB002163

Wang YL, Yan P, Zheng HB, Lu XY (2007) Timing and positioning corrections of ocean bottom seismograph data. J Trop Oceanogr 26(05):40–46

Watremez L, Helen Lau KW, Nedimović MR, Louden KE (2015) Traveltime tomography of a dense wide-angle profile across Orphan Basin. Geophysics 80(3):B69–B82. https://doi.org/10.1190/geo2014-0377.1

Xue B, Ruan AG, Li XY, Wu ZL (2008) The seismic data corrections of short period auto-floating ocean bottom seismometer. J Mar Sci 26(2):98102

Yasukawa H, Sakuno R (2020) Application of the MMG method for the prediction of steady sailing condition and course stability of a ship under external disturbances. J Mar Sci Technol 25(1):196–220

Zhang G, Zhang C, Xie Z (2013) A decision making support system for ocean-bottom seismometer position based on GIS. Proc Comput Sci 18:2454–2457. https://doi.org/10.1016/j.procs.2013.05.421

Zhao M, Du F, Wang Q, Qiu X, Fan C (2018) Current status and challenges for three-dimensional deep seismic survey in the south china sea. Earth Sci 43(10):3749–3761. https://doi.org/10.3799/dqkx.2018.573